Statistical Characteristics of Environmental Parameters for Warm Season Short-Duration Heavy Rainfall over Central and Eastern China

TIAN Fuyou[1,2,3] (田付友), ZHENG Yongguang[3*] (郑永光), ZHANG Tao[3] (张 涛), ZHANG Xiaoling[3] (张小玲), MAO Dongyan[3] (毛冬艳), SUN Jianhua[1,2] (孙建华), and ZHAO Sixiong[1,2] (赵思雄)

1 *Key Laboratory of Cloud-Precipitation Physics and Severe Storms, Institute of Atmospheric Physics, Chinese Academy of Sciences, Beijing* 100029

2 *University of Chinese Academy of Sciences, Beijing* 100049

3 *National Meteorological Center, China Meteorological Administration, Beijing* 100081

(Received August 23, 2014; in final form February 26, 2015)

ABSTRACT

Water vapor content, instability, and convergence conditions are the key to short-duration heavy rainfall forecasting. It is necessary to understand the large-scale atmospheric environment characteristics of short-duration heavy rainfall by investigating the distribution of physical parameters for different hourly rainfall intensities. The observed hourly rainfall data in China and the NCEP final analysis (FNL) data during 1 May and 30 September from 2002 to 2009 are used. NCEP FNL data are 6-hourly, resulting in sample sizes of 1573370, 355346, and 11401 for three categories of hourly rainfall (P) of no precipitation ($P < 0.1$ mm h^{-1}), ordinary precipitation ($0.1 \leqslant P < 20$ mm h^{-1}), and short-duration heavy rainfall ($P \geqslant 20.0$ mm h^{-1}), respectively, by adopting a temporal matching method. The results show that the total precipitable water (PWAT) is the best parameter indicating the hourly rainfall intensity. A PWAT of 28 mm is necessary for any short-duration heavy rainfall. The possibility of short-duration heavy rainfall occurrence increases with PWAT, and a PWAT of 59 mm is nearly sufficient. The specific humidity is a better indicator than relative humidity. Both 700- and 850-hPa relative humidity greater than 80% could be used to determine whether or not it is going to rain, but could not be used to estimate the rainfall intensity. Temperature and potential pseudo-equivalent temperature are also reasonable indicators of short-duration heavy rainfall. Among the atmospheric instability parameters, the best lifted index (BLI) performs best on the short-duration rainfall discrimination; the next best is the K index (KI). The three rainfall categories are not well recognized by total totals (TT) or the temperature difference between 850 and 500 hPa (DT85). Three-quarters of short-duration heavy rainfall occurred with BLI less than –0.9, while no short-duration heavy rainfall occurred when BLI was greater than 2.6. The minimum threshold of KI was 28.1 for short-duration heavy rainfall. The importance of dynamic conditions was well demonstrated by the 925- and 850-hPa divergence. The representativeness of 925-hPa divergence is stronger than that of 850 hPa. Three-quarters of short-duration heavy rainfall occurred under a negative divergence environment. However, both the best convective potential energy (BCAPE) and vertical wind shear were unable to discriminate the hourly rainfall intensities.

Key words: short-duration heavy rainfall, parameter, statistic characteristics, atmosphere environment

Citation: Tian Fuyou, Zheng Yongguang, Zhang Tao, et al., 2015: Statistical characteristics of environmental parameters for warm season short-duration heavy rainfall over central and eastern China. *J. Meteor. Res.*, **29**(3), 370–384, doi: 10.1007/s13351-014-4119-y.

Supported by the Meteorological Integration and Application of Key Techniques (CMAGJ2013Z04), China Meteorological Administration Special Public Welfare Research Fund (GYHY201406002 and GYHY201206004), and National (Key) Basic Research and Development (973) Program of China (2013CB430106).

*Corresponding authors: zhengyg@cma.gov.cn.

1. Introduction

Rainstorms are one of the most severe weather events in China. The area hit by rainstorms in a given year is often on the order of 100000 km^2. An average of 53 disasters caused directly by rainstorms was reported annually during 1852–1982 (Lu and Yang, 2000). Though flooding is usually caused by persistent precipitation or high intensity short-duration heavy rainfall, the latter is more familiar to city dwellers and is more destructive. For example, during the Beijing extreme rainfall event of 21 July 2012, hourly rainfall of 100.3 mm was reported, and it left great damage. Therefore, improving the accuracy of short-duration heavy rainfall prediction is vital for disaster prevention and reduction.

A short-duration heavy rainfall is a reported hourly rainfall accumulation of more than 20.0 mm at the National Meteorological Center, China Meteorological Administration. Most of the short-duration heavy rainfalls form directly from meso- and microscale systems with a short life-cycle, a small spatial scale, and drastic changes of atmospheric elements. Short-term forecasting and nowcasting could use extrapolation technology developed from remote sensing results (Wilson et al., 1998). However, due to the limitation of extrapolation techniques, prediction of storm generation, extinction, and development is difficult. Short- and mid-term forecasts must be based on numerical prediction models. Due to the limitation of data assimilation, imperfect parameterization processes, model resolution, and so on (Boville, 1991; Molinari and Dudek, 1992; Arakawa, 2004; Yu and Lee, 2010), many global and mesoscale numerical prediction models cannot accurately forecast short-duration heavy rainfall, especially warm sector convective precipitation (Fritsch and Carbone, 2004). At present, the prediction of short-duration heavy rainfall produced by mesoscale systems is the combination of subjective and objective techniques.

Based on the scientific understanding of heavy precipitation, Doswell et al. (1996) proposed an "ingredients-based" methodology to forecast flash floods. We know that multi flash flood-producing storms most probably come from similar environment conditions. Some of these conditions, such as instability and moisture, can be characterized by physical quantities and parameters. Wetzel and Martin (2001) successfully applied this idea to a midlatitude winter precipitation forecast.

With the application of the "ingredients-based" methodology, an exact understanding of the physical quantities and indices under different synoptic patterns is critically important. Fortunately, a solid foundation has been established by the U.S. storm prediction center. Miller (1972) provided a detailed introduction of the application of parameters and indices to forecast categorized severe convective weather phenomena. Rasmussen and Blanchard (1998) carefully examined the parameters of non-supercell thunderstorms, supercells without significant tornadoes, and supercells with significant tornadoes, showing how combined parameters could strongly discriminate between the environments. Further, Rasmussen (2003) provided three modified forecast parameters for distinguishing the environment favorable for significant tornadoes and large hail but no significant tornadoes. A comparison completed by Thompson et al. (2012) showed that measures of buoyancy could be best used to discriminate between supercell and quasi-linear convective system tornado events during the winter. All these studies provide documented materials for the U.S. forecast of tornadoes, hail and thunderstorm winds. However, a study carried out by Lin et al. (2001) showed that the high convective available potential energy (CAPE) value typically observed in East Asian cases is not consistently observed in similar cases in the U.S. and Europe, indicating that the environmental conditions differ. A comparison of physical properties, derived from the environmental soundings of mesoscale convective systems, between different studies for the U.S. and China shows that the environment is much wetter in China than in U.S. (Zheng et al., 2013). Therefore, the environmental conditions expressed by same parameters may differ greatly for different areas. Correct choice and application of parameters based on thermodynamic and dynamic parameters is vitally important to accurate forecasting

of convective weather.

Zhang et al. (2012) and Zhang et al. (2013) documented that the "ingredients-based" methodology could be successfully applied to the operational forecast of categorized severe convective weather by recognizing the environment. Some preliminary studies recognized environmental facilitation for different severe convective weather in China (Lei et al., 2011; Sun et al., 2014). Li et al. (2004) discussed a possible approach of convective weather forecasting with dynamic and energetic parameters. Zhang et al. (2012) provided a qualitative analysis of the atmosphere environmental conditions facilitating convective weathers. Fan and Yu (2013) revealed with sounding data that, compared to hails and thunderstorms, the temperature difference between 850 and 500 hPa is smaller for those generating only short-duration heavy rainfall, and the vertical wind shear is weaker. Using 2-yr sounding data, Lei et al. (2011) studied the significance of parameters on distinguishing the category of the summer convective weather in Beijing. An experimental study of the summer convective weather categorical probability forecast based on the rapid updated cycle system for the Beijing area (BJ-RUC) was carried out by Lei et al. (2012), and the results showed that the prediction ability of convective weather of BJ-RUC could be significantly improved.

Though these studies provide very useful information on the application of thermodynamic and dynamic parameters by characterizing the environment conditions favorable for different convective weather, critical thresholds and detailed parameter distributions for a specific convective weather phenomenon, especially short-duration heavy rainfall, are still needed. Further, we still know few about necessary or sufficient thresholds for specific convective weather types, especially short-duration heavy rainfall, which limits the interpretation and application of the parameters. Some case studies (e.g., Li and Li, 2000; Qian et al., 2007; Yin et al., 2010) use ambiguous words such as "strong", "moderate" to describe the environmental conditions through estimating parameter values such as CAPE, K index (KI), and so on. These words are obscure, subjective, and experience-based, and limit case study inter-comparison. Objective description and specific thresholds of many parameters are urgently needed.

Based on the physical mechanism and environment conditions of short-duration heavy rainfall, several parameters indicating the moisture, instability, and lifting conditions of the environment are statistical analyzed by comparing the distribution of non-precipitation, ordinary precipitation, and short-duration heavy rainfall. The significance and thresholds of parameters for short-duration heavy rainfall are objectively described, and necessary and sufficient thresholds are provided. All these are necessary for the subjective forecasting and statistical-dynamic based prediction of short-duration heavy rainfall.

2. Data analysis

The quality controlled hourly rainfall data from 1991 to 2009 were obtained from the National Meteorological Information Center. The start date for the stations differed due to the climatology and construction of observational instruments. The stations located in southern China had records for the whole year, while those in the north only had records from the warmer months of May to September. Short-duration heavy rainfall in China mainly occurred during the warm season, according to Chen et al. (2013) and Tian et al. (2014). Records beginning later than 1 May or ending earlier than 30 September were rejected. Questionable records were also rejected according to their identification code provided along with the data. Following this process, 411 stations remained. However, only the National Centers for Environmental Prediction Final Analysis (NCEP FNL) data from 2002 to 2009 were available; and the NCEP FNL data and hourly rainfall data needed to match, the hourly rainfall data during this period were ultimately used.

According to the definition of short-duration heavy rainfall, the hourly rainfall (P) data are divided into non-precipitation ($P < 0.1$ mm h^{-1}), ordinary precipitation ($0.1 \leqslant P < 20.0$ mm h^{-1}), and short-duration heavy rainfall ($P \geqslant 20.0$ mm h^{-1}). The study carried out by Tian et al. (2014) showed that

the probability of short-duration heavy rainfall decreases rapidly as the altitude increases. The distribution of short-duration heavy rainfall from 2002 to 2009 during 1 May and 30 September (Fig. 1) shows that the frequency decreases from the coastal area of South China to Northeast China. The frequency of short-duration heavy rainfall is more than 200 over the coastal areas of South China. The frequency over North China is between 10 and 80. Over Northeast China, the frequency is rarely more than 80. This distribution is in good agreement with the topography (Fig. 2). The used stations are those located in central and eastern China, with an altitude of 1000 m or less as shown in Fig. 2.

The parameters used in this study are obtained from the NCEP FNL 6-hourly data with a horizontal resolution of 1° × 1°. The NCEP FNL data are used to represent the atmosphere environment instead of soundings for three reasons. (1) Short-duration heavy rainfall mainly occurs in the afternoon (Chen et al., 2013), whereas soundings are launched twice daily (at 0000 and 1200 UTC), so the data are too sparse. (2) The synoptic patterns are well characterized by the NCEP FNL data over central and eastern China (Huang, 2006; Zhao and Wu, 2007). (3) Due to the different natures of sounding and NCEP FNL, there must be some differences for the results obtained from sounding and NCEP FNL. However, a comparison completed by Wang et al. (2012) showed that some of the quantities, such as KI and wind field, could be well represented by the NCEP FNL data.

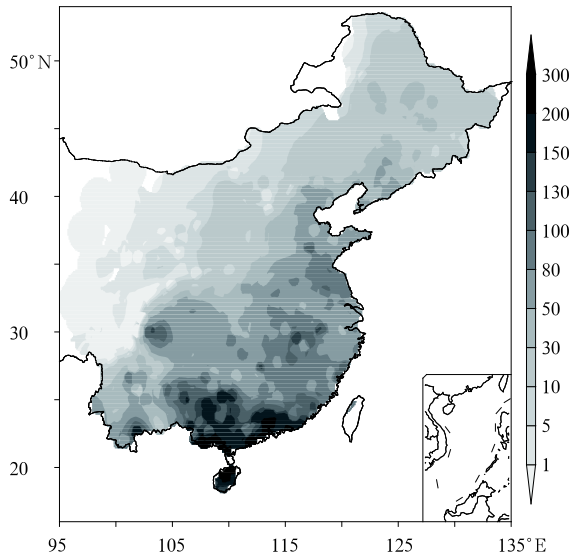

Fig. 1. Frequency of short-duration heavy rainfall during 1 May and 30 September from 2002 to 2009.

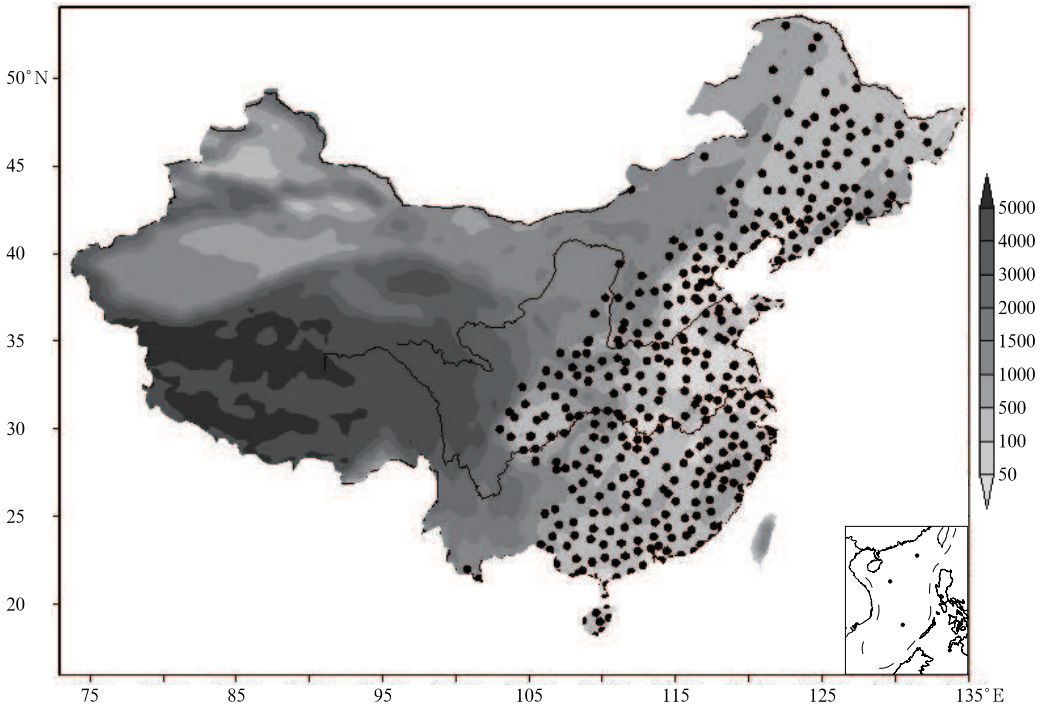

Fig. 2. Distribution of the 411 stations. The shadings indicate topography (m).

The NCEP FNL data are gridded while the observational data are irregularly scattered, so the former were interpolated onto the stations. However, to process the observations, a proximity method was adopted. The NCEP FNL data times have 0000, 0600, 1200, and 1800 UTC as centers. Thus, there are six records for a single period per station with 0000, 0600, 1200, and 1800 UTC as centers. For these six records, the maximum value was identified and considered as the hourly precipitation corresponding to the NCEP FNL data. Using the previously described process, the sample sizes of non-precipitation, ordinary precipitation, and short-duration heavy rainfall are 1573370, 355346, and 11401, respectively.

3. Characteristics of environmental parameters

Severe convective weather requires moisture, instability, lifting, and vertical wind shear. The results thought to be highly related to short-duration heavy rainfall are characterized. Table 1 lists the parameters used in this study. A detailed description of the parameters is given in Appendix.

Table 1. Parameter abbreviations and their units

Name	Abbreviation	Unit
Total precipitable water	PWAT	mm
Specific humidity	q	g kg^{-1}
Temperature difference between 850 and 500 hPa	DT85	℃
Best lifted index	BLI	℃
Total totals	TT	℃
K index	KI	℃
Best convective available potential energy	BCAPE	J kg^{-1}
Divergence	DIV	s^{-1}
Vertical wind shear	SHR	m s^{-1}

Moisture is represented by the total precipitable water (PWAT), and the specific humidity (q) at 925, 850, and 700 hPa. The saturation level is represented by the relative humidity at 850 and 700 hPa. The prerequisite of temperature at 850 and 925 hPa, and the potential pseudo-equivalent temperature, the combination of moisture and instability, are also analyzed. The parameters used to denote the atmosphere instabilities are the best lifted index (BLI), the total totals (TT), KI, and the temperature difference between 850 and 500 hPa (DT85). The ascent is indicated by the 850- and 925-hPa divergence. The widely used best convective available potential energy (BCAPE) is also analyzed. The magnitude of wind shear is the average wind shear between 0 and 1 km (SHR1), 0 and 3 km (SHR3), and 0 and 6 km (SHR6).

3.1 Moisture conditions

Moisture is a requirement of severe convective weather. The impact of water vapor on buoyancy is affected by many microphysics processes, and free-tropospheric moisture plays a key role in the transition from shallow to deep convection (Holloway and Neelin, 2009). For the moisture related parameters, the PWAT is the approximation of the actual water vapor content in the volume air unit, i.e., water vapor integrated from the land surface to 200 hPa. It is the absolute water content in the atmosphere. Specific humidity, comparable to the mixing ratio, is the absolute water content of specific pressure levels. Relative humidity denotes the saturation level of the atmosphere. To estimate the absolute water content by using relative humidity, we have to know the temperature of the atmosphere.

Figure 3 shows box-and-whisker plots of PWAT for the three hourly rainfall categories. The ranges of PWAT are 6–65, 14–70, and 28–74 mm, respectively. With increasing intensity, the 99th percentile differs little, while the 1st percentile doubled. The 1st percentile of non-precipitation PWAT indicates that PWAT in the atmosphere is always larger than 6 mm. However, if liquid water reaches the ground and is recorded by rain gauges, the PWAT should not be less than 14 mm. For short-duration heavy rainfall, the PWAT should not be less than 28 mm. With a PWAT of less than 28 mm, even stronger lifting and instability exists, short-duration heavy rainfall is rarely observed. The difference of the 1st percentile of non-precipitation and short-duration heavy rainfall is about 22 mm, close to the threshold of short-duration heavy rainfall of 20.0 mm. This value is consistent with the threshold of different rainfall intensities given by Humphreys (1919). The significance of this result is that a 28-mm PWAT is necessary for short-duration heavy rainfall.

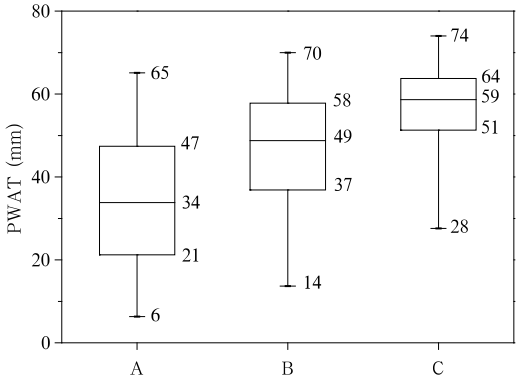

Fig. 3. Box-and-whisker plots for the PWAT of the three rainfall categories. The upper and lower horizontal bars represent the 99th and the 1st percentile of the PWAT distribution, while the three horizontal lines of the boxes indicate the 75th, 50th (median), and 25th percentiles, respectively. A, B, and C indicate no rain ($P < 0.1$ mm h^{-1}), ordinary precipitation ($0.1 \leqslant P < 20.0$ mm h^{-1}), and short-duration heavy rainfall ($P \geqslant 20.0$ mm h^{-1}).

From Fig. 3, we see that the box-and-whisker plot is near uniformly distributed for non-precipitation. The ordinary precipitation concentrates in the upper 50 percentiles. The possibility of short-duration heavy rainfall increases with PWAT. Three-quarters of short-duration heavy rainfall occurred with PWAT larger than 51 mm. With this threshold, the ordinary precipitation is about 50%, and non-precipitation is about 25%. It indicates that the larger the amount of moisture, the higher the probability of short-duration heavy rainfall. The median value for short-duration heavy rainfall is 59 mm. However, less than 25% of ordinary precipitation events have a PWAT in excess of 59 mm, and non-precipitation is far less than 25% when the PWAT is greater than 59 mm. A PWAT greater than 70 mm is sufficient for short-duration heavy rainfall, as only a very small proportion of non-precipitation and ordinary precipitation occurred then. A PWAT larger than 70 mm is rarely observed, and short-duration heavy rainfall meeting this threshold is rarely reported.

Every pressure level has its own specific humidity. From Fig. 4, we see that the distribution of q for the three pressure levels is the same as PWAT, though the q for lower pressure levels is larger than that for higher pressure levels for the same percentiles. The median of q for the three hourly rainfall categories are 11.4, 14.0, and 16.8 g kg^{-1} for 925 hPa, respectively. The first quartile for short-duration heavy rainfall is 15.4 g kg^{-1}. The ordinary precipitation excess this threshold is less than 50%, and for non-precipitation is about 25%. For the median of 16.8 g kg^{-1} for short-duration heavy rainfall, the ordinary precipitation excess this threshold is less than 25%, and for non-precipitation, it is far less than 25%. Similar characteristics for other pressure levels are presented in Fig. 4.

The significance of the 1st percentile's specific humidity of 8.8, 7.7, and 4.5 g kg^{-1} for 925, 850, and 700 hPa is that if one does not meet the threshold, then short-duration heavy rainfall is not be expected. The absolute moisture content, characterized by q of 925, 850, and 700 hPa, should not less than 8.8, 7.7, and 4.5 g kg^{-1}, respectively. Specific humidity of 16.8, 14.3, and 9.8 g kg^{-1} is considered approximately sufficient conditions for short-duration heavy rainfall.

Relative humidity is the ratio of the partial pressure of water vapor to the equilibrium vapor pressure of water at the same temperature. The same relative humidity may result in completely different phenomena during different seasons. Here only the relative humidity at 850 and 700 hPa is analyzed. Non-precipitation can happen in almost any relative humidity environment, as shown in Fig. 5. However, for both ordinary precipitation and short-duration heavy rainfall, 75% of events occur with a relative hu-

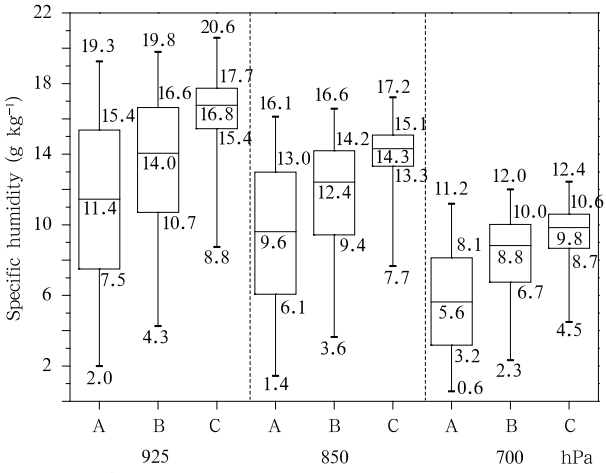

Fig. 4. As in Fig. 3, but for 925-, 850-, and 700-hPa specific humidity.

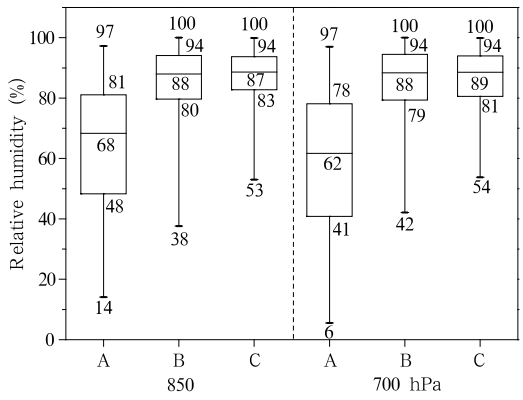

Fig. 5. As in Fig. 3, but for 850- and 700-hPa relative humidity.

midity greater than 80% for both 850 and 700 hPa. Air with relative humidity less than 50% is very dry, while that greater than 65% is moist (Miller, 1972). From Fig. 5, we can see that the non-precipitation occurring in dry and wet environments is about half and half. But for ordinary precipitation and short-duration heavy rainfall about 75% of events occur in the wet conditions with a relative humidity higher than 80%. Relative humidity does not aid recognition of short-duration heavy rainfall from ordinary precipitation. It can be concluded that a relative humidity greater than 50% is necessary for short-duration heavy rainfall, but even a 100% relative humidity could not predict a short-duration heavy rainfall event with certainty. Precipitation forms in a saturated atmosphere, so a relative humidity during precipitation less than 50% may arise from the restricted resolution of the observational and FNL data.

The temperature near the land surface determines the possible maximum air water content. The pseudo-equivalent potential temperature is a parameter frequently used during operations. The 850- and 925-hPa temperature and pseudo-equivalent potential temperature are analyzed to demonstrate their effectiveness in indicating hourly rainfall intensities.

The rainfall intensities are not well distinguished by either the temperature at 850 or 925 hPa (Fig. 6a) as the same percentiles for different rainfall intensities high and low intersect. The variation range of temperature for short-duration heavy rainfall is smaller compared to the other two types. Half of short-duration heavy rainfall events occur with a 925-hPa temperature between 21.7 and 24.3℃, while the 850-hPa temperature between 18.0 and 20.0℃. However, the 99th percentile of the 925- and 850-hPa temperatures for short-duration heavy rainfall is 29.2 and 23.5℃, respectively. 99% of short-duration heavy rainfall events have 925- and 850-hPa temperatures greater than 16.0 and 12.1℃, respectively. The 1st percentile of 925- and 850-hPa temperatures represents the necessary temperature for short-duration heavy rainfall over central and eastern China. According to the temperature climatology provided by Zhang and Lin (1985), extensive short-duration heavy rainfall first occurs over southern China during April, and disappears after October. This is in good agreement with the climatology of short-duration heavy rainfall (Chen et al., 2013).

The potential pseudo-equivalent temperature is a

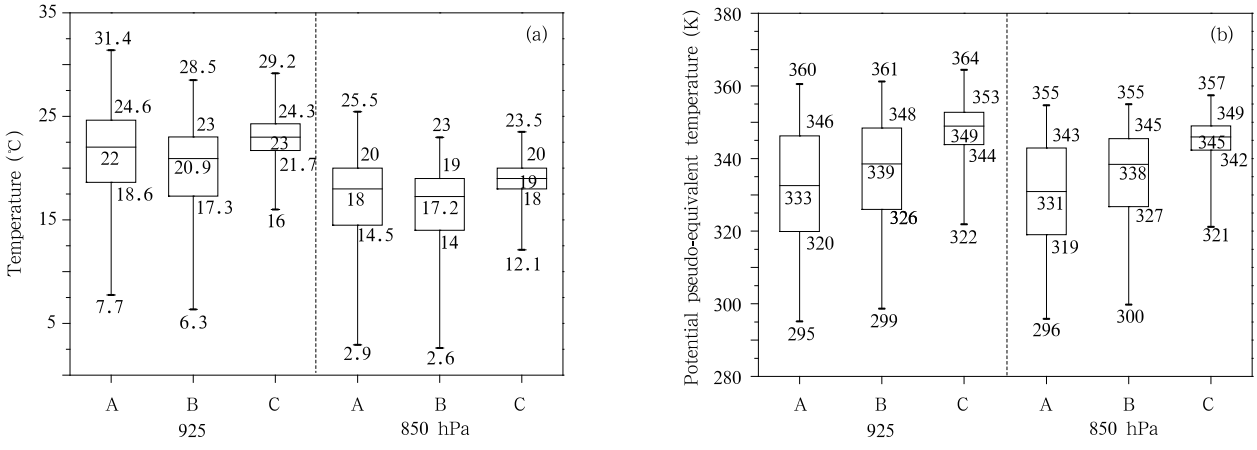

Fig. 6. As in Fig. 3, but for (a) temperature and (b) potential pseudo-equivalent temperature at 925 and 850 hPa.

better indicator than temperature, as it takes moisture into consideration. The ranges of values are 322–364 and 321–357 K for 925 and 850 hPa, respectively. The medians for the two pressure layers are 349 and 346 K, respectively. For both non-precipitation and ordinary precipitation, the potential pseudo-equivalent temperature greater than the median of short-duration heavy rainfall for the pressure layers of 925 and 850 hPa is less than 25%. Therefore, the essential potential pseudo-equivalent temperature of both 925 and 850 hPa for short-duration heavy rainfall is about 321 K. A potential pseudo-equivalent temperature of 925 hPa (850 hPa), greater than 353 K (349 K), is approximately sufficient for short-duration heavy rainfall as the percentage of non-precipitation and ordinary precipitation excess this threshold is far less than 25%.

The results show that relative humidity can only help determine whether it is raining, while PWAT, specific humidity, and potential pseudo-equivalent temperature also indicate rainfall intensity. However, the 925- and 850-hPa temperatures could not be used to distinguish possible rainfall intensities.

Figure 3 shows that the median ordinary precipitation (49 mm) and the 75% percentile of non-precipitation (47 mm) are very close, and the median of short-duration heavy rainfall (59 mm) and the 75% percentile of ordinary precipitation (58 mm) are also close for PWAT. The same characteristic is presented with specific humidity in Fig. 4. Whether these distributions are coincidence or determined by physical conditions on precipitation formation is unknown.

Both PWAT and low level specific humidity are better at recognizing environmental moisture conditions favorable for short-duration heavy rainfall compared to other parameters. However, it is difficult to judge which is better by using the box-and-whisker plots. The distribution of relative frequency and the cumulative density function (CDF) of PWAT and q for the three rainfall categories are given (Fig. 7). From Fig. 7a, we can see that a maximum relative frequency appears with a PWAT of 25 mm, and that the relative frequency of non-precipitation decreases with the increase of PWAT. However, the relative frequency of ordinary precipitation increases with the increase of PWAT: PWAT reaches its maximum of 6.0% at the value of 60 mm. For short-duration heavy rainfall, the maximum relative frequency reaches a maximum of 10.5% with a PWAT of 64 mm. This is in agreement with the results shown by the box-and-whisker plots. Non-precipitation can occur with any PWAT. However, when PWAT exceeds certain thresholds, the proportion drops quickly. Short-duration heavy rainfall events only occurred with a PWAT greater than 28 mm, and a more rapid growth rate, compared to ordinary precipitation. It could be more significantly displayed by the CDF. The farther the distance between the peak points of the relative frequencies, the better the differentiation of rainfall intensities. Only the 925-hPa specific humidity (Fig. 7b) is given, as the distribution of different pressure layers is much

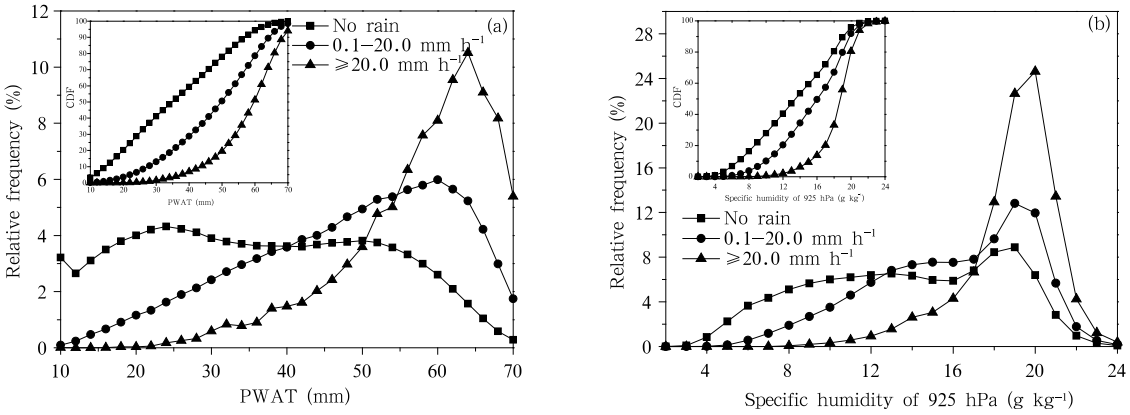

Fig. 7. Relative frequency (%) and cumulative distribution function (CDF) distribution of parameters used to denote the atmospheric water vapor conditions. (a) PWAT (mm) and (b) 925-hPa q (g kg^{-1}). The CDF is shown in the top left corner insets.

the same. However, though the rainfall intensities are well distinguished by the CDF, the relative frequencies all reach their maximum at the same specific humidity of 20.0 g kg^{-1}. This may be due to the importance of the total water vapor content for short-duration heavy rainfall. Most air moisture concentrates in the lower atmosphere, but the formation of short-duration heavy rainfall requires not only the moisture in the lower atmosphere, but also the total air moisture represented by PWAT.

3.2 Instability conditions

There are a few parameters used to represent atmospheric instability. Only the BLI, KI, TT, and DT85 are studied here. A negative BLI represents atmospheric instability. From this perspective, the BLI is most easy to identify by the sign.

Figure 8 shows box-and-whisker plots of the parameters representing atmospheric instability. The BLI, KI, and TT have similar distributions. The median increases remarkably with increasing rainfall intensity for the same parameter. The medians of DT85 for the three rainfall intensities is staggered. The medians for the three rainfall intensities of BLI are 1.1, 0.0, and –2.0; for KI are 27.8, 34.5, and 37.7; for TT are 42, 42, and 44; and for DT85 are 24, 22, and 23, respectively. The median of TT for the three rainfall intensities is too close.

The median of BLI for ordinary precipitation is 0.0, indicating that ordinary precipitation events occur equally in stable and unstable environments. For short-duration heavy rainfall, the 75% percentile is –0.9, indicating that 75% of events occur in an instable environment. However, about a quarter of short-duration heavy rainfall events occur under a stable environment represented by BLI. The distribution of KI is similar to BLI. Half of ordinary precipitation events occur with a KI larger than 34.5, while this is less than 25% for non-precipitation, and for short-duration heavy rainfall greater than 75%. However, compared to the range of 12.6–41.2 of KI for ordinary precipitation, the range for short-duration heavy rainfall is 28.1–42.2, and more than 75% of events have a KI larger than 36.0.

The distribution of relative frequency and CDF of BLI and KI is also shown in Fig. 9. The relative

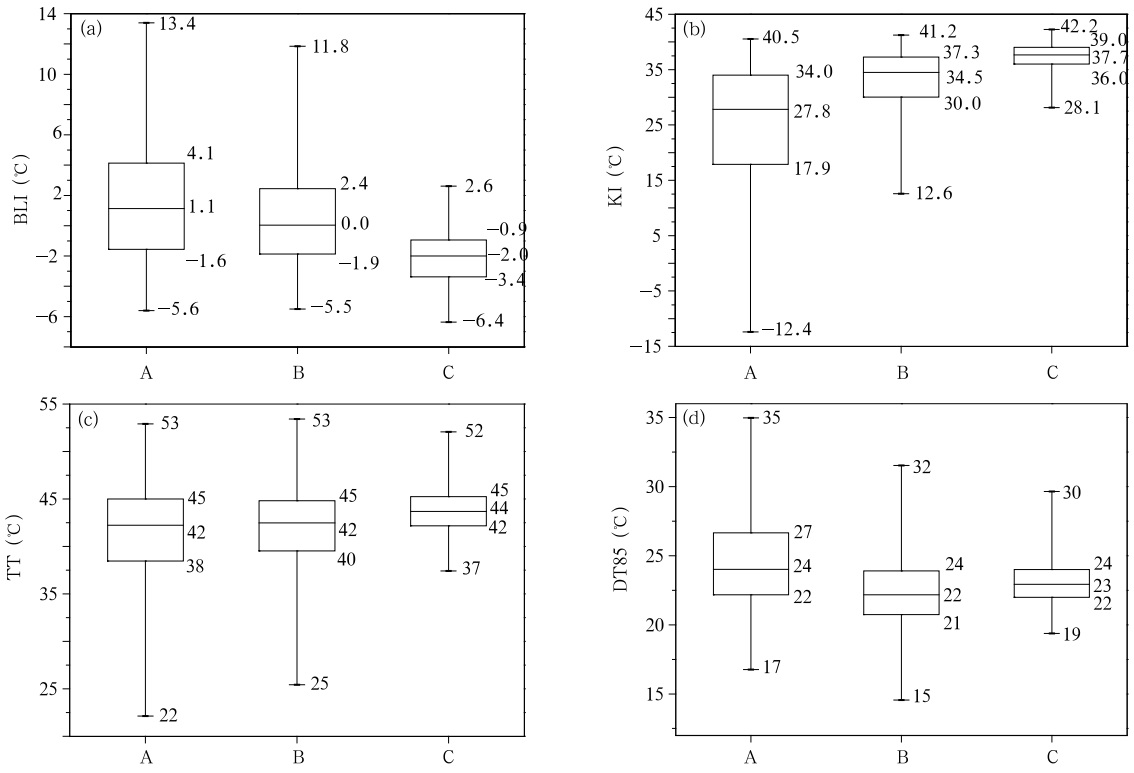

Fig. 8. As in Fig. 3, but for atmospheric instability. (a) BLI, (b) KI, (c) TT, and (d) DT85.

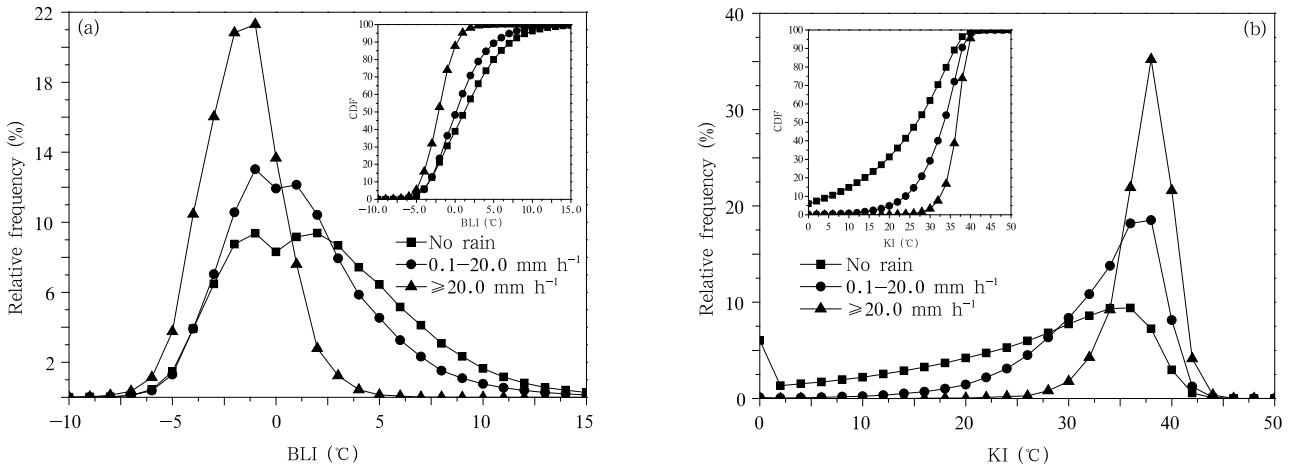

Fig. 9. Distribution of relative frequency (%) for (a) BLI and (b) KI. The CDF is shown in the top corner.

frequencies show that the BLI peaks for both non-precipitation and ordinary precipitation are about 0.0, but for short-duration heavy rainfall the peak is –2.0. For KI the peaks are 36.0, 36.0, and 38.0, respectively. The denotative meaning is similar. The CDFs show that KI can better distinguish short-duration heavy rainfall from non-precipitation and ordinary precipitation. However, the environmental stability could be characterized by using the BLI sign, which is perhaps more intuitive. The environmental instability represented by BLI or KI should not be greater than 2.6 or larger than 28.1, respectively. Generally speaking, the BLI should be negative during convective weather. A positive BLI during short-duration heavy rainfall may arise from the spatial and temporal resolution, as mesoscale systems could not be completely represented by parameters obtained from global numerical prediction models.

CAPE represents the possible upwards buoyancy force. A study on the relationship between convective activity and stability carried by McBride and Frank (1999) showed that convective activity is weakly but inversely related to CAPE variations. Variation in convective activity is related to moisture content. However, Peppler and Lamb (1989) found that summer rainfall over the U.S. is better correlated with the humidity of air just above the boundary layer than with CAPE values of air within the boundary layer.

The warm season rainfall intensity in central and eastern China could not be well identified by BCAPE as shown in Fig. 10. The box-and-whisker plots of BCAPE for the three rainfall intensities show that about half of non-precipitation and ordinary precipitation events occur with a BCAPE of 0 J kg^{-1} (Fig. 10). Though more than 75% of short-duration heavy rainfall events are accompanied with certain BCAPE, there are still more than 75% of non-precipitation and ordinary precipitation events occur with a certain amount of BCAPE, and about 25% short-duration heavy rainfall events occur with no BCAPE. The median of BCAPE for short-duration heavy rainfall is 629.0 J kg^{-1}, which is not as remarkable as that in the environment reorganization of tornadoes in the U.S. (Thompson et al., 2012). The reason may be the same as BLI, which is caused by the incomplete representation of the environmental parameters obtained from global numerical prediction models.

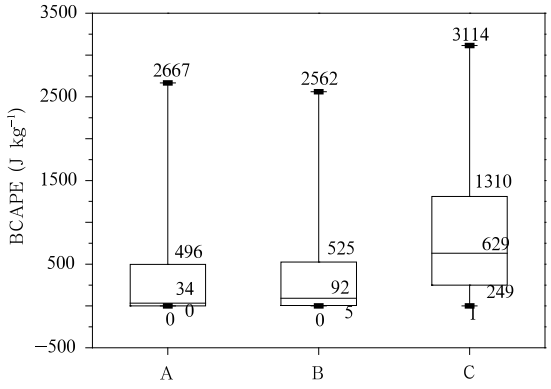

Fig. 10. As in Fig. 3, but for BCAPE.

3.3 Dynamic conditions

The triggers of convective activities are usually boundary layer convergence such as shear lines, fronts, and sea breezes (Fankhauser et al., 1995). Here the large-scale divergence was considered a convective system trigger, and mesoscale systems were ignored. Watson and Blanchard (1984) documented the total area divergence, and noted its relation to area rainfall. A correlation coefficient of 0.75 between the change in divergence and the rainfall amount was found for the 75 rain events during the Florida area cumulus experiment in 1975. The maximum rain could occur 38 minutes before peak convergence, or hours later after maximum convergence.

Figure 11 shows box-and-whisker plots of 925- and 850-hPa divergence for the three rainfall intensities. We can see that, with the increase of rainfall intensity, the portion of rain with negative divergence increases, denoting an enhancement of divergence. For non-precipitation, the median of both 925- and 850-hPa divergence is close to 0. More than 50% of ordinary precipitation events occur with a negative divergence. For short-duration heavy rainfall the percentage is about 75%. It is apparent that ascent produced by environmental convergence is necessary for short-duration heavy rainfall. It is not always clear from which layer the ascent begins. By comparing the divergence of 925 and 850 hPa and using the smaller one, the box-and-whiskers plots shown as DIV are given. Compared to the distributions of the 925- and 850-hPa divergence, far more than 75% of short-duration heavy rainfall events occur with a negative DIV, while the percentages for ordinary precipitation and non-precipitation are about 25% and 50%, respectively. The larger the rainfall intensity, the more divergence required. Thus, divergence should be carefully analyzed to determine potential areas of short-duration heavy rainfall.

There is consensus regarding vertical wind shear in convective storms such as supercells (Bunkers, 2002; Zhang et al., 2012). It is commonly thought that strong vertical wind shear is unfavorable for torrential rain (Ding, 2005). Figure 12 shows a box-and-whisker plot of SHR1, SHR3, and SHR6 for the three rainfall intensities. However, the medians are all close for the three rainfall intensities, no matter the vertical wind shear. For example, the median of SHR1 for ordinary precipitation is larger than that for non-precipitation, but also larger than that for short-duration heavy rainfall. Vertical wind shear could help recognize rainfall intensities different to those in severe convective storms (Weisman and Klemp, 1982). However, a certain value of SHR1 is favorable for precipitation compared to SHR3 and SHR6. This may be related to a low level jet moisture transform frequently reported over monsoon areas. Strong vertical wind shear is not favorable for short-duration heavy rainfall.

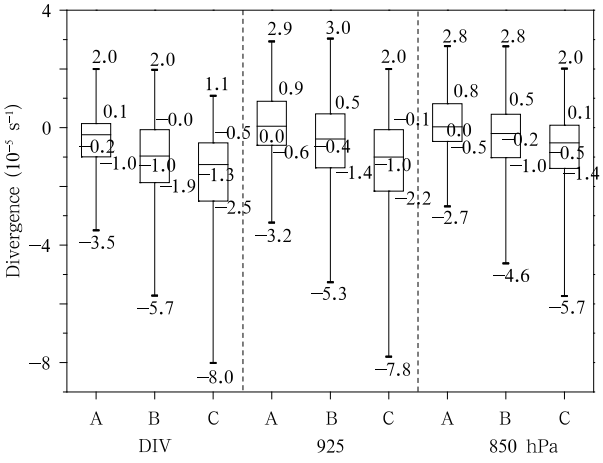

Fig. 11. As in Fig. 3, but for divergence at 925 and 850 hPa. DIV is the distribution of strongest divergence between 925 and 850 hPa for the same hourly rainfall.

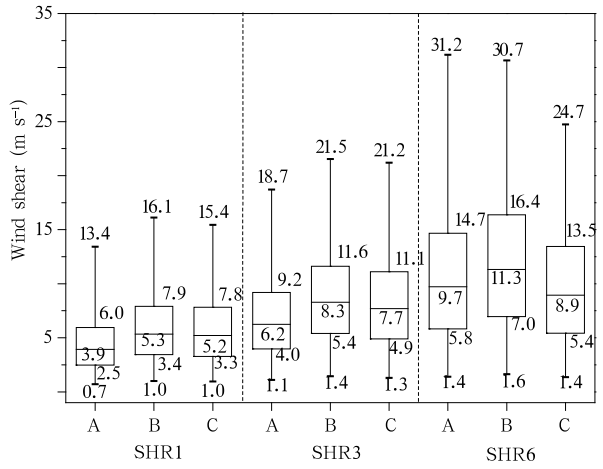

Fig. 12. As in Fig. 3, but for SHR1, SHR3, and SHR6.

3.4 A summary of parameters favorable for short-duration heavy rainfall

The distributions of parameters for non-precipitation, ordinary precipitation, and short-duration heavy rainfall show that a certain amount of moisture, instability, and ascent is necessary for short-duration heavy rainfall. For the moisture related parameters, PWAT and specific humidity are good indicators. Values of 28 and 59 mm are necessary and near sufficient, respectively. An area with PWAT less than 28 mm is unlikely to have short-duration heavy rainfall while PWAT larger than 59 mm indicates a high possibility. Specific humidity at 925, 850, and 700 hPa should be greater than 8.8, 7.7, and 4.5 g kg^{-1} for short-duration heavy rainfall. Specific humidity of 925, 850, and 700 hPa greater than 16.8, 14.3, and 9.8 g kg^{-1} could be considered as near sufficient conditions. BLI and KI are good indicators for environmental instability compared to other indices. A short-duration heavy rainfall is likely with a BLI less than 2.6 or KI greater than 28.1. Divergence of 925 or 850 hPa should not be greater than 2.0×10^{-5} s^{-1}. High atmospheric temperature is the precondition of high moisture content. Central and eastern China, controlled by the summer monsoon, is hot and humid. This kind of air is extremely unstable, and always favorable for convective activities. Meanwhile, PWAT is always high, thus short-duration heavy rainfall is frequently reported. Some of the thresholds of important parameters are listed in Table 2, which can be used as a reference during operational forecasting of short-duration heavy rainfall.

Table 2. Thresholds of some indicative parameters used for short-duration heavy rainfall forecasting

Parameters	PWAT	925-hPa q	850-hPa q	BLI	KI	T850	T925	DIV925	DIV850
Necessary	$\geqslant 28$	$\geqslant 8.8$	$\geqslant 7.7$	$\leqslant 2.6$	$\geqslant 28$	$\geqslant 12.1$	$\geqslant 16.0$	$\leqslant 2.0\times10^{-5}$	$\leqslant 2.0\times10^{-5}$
The 75th percentile	64	17.7	15.1	–3.4	39.0	24.3	20	-2.2×10^{-5}	-1.4×10^{-5}
The 99th percentile	74	20.6	17.2	–6.4	42.2	29.2	23.5	-7.8×10^{-5}	-5.7×10^{-5}

4. Conclusions and discussion

Prediction of short-duration heavy rainfall is a complex process, during which the distribution and magnitude of the moisture, lifting mechanism, and atmospheric instability should all be considered. No single parameter alone may be used to make an accurate prediction. However, knowledge of key thresholds of necessary and near sufficiency of parameters could help determine which regions should be most closely focused on during the flood seasons, so that short-duration heavy rainfall can be estimated.

The distributions of non-precipitation, ordinary precipitation, and short-duration heavy rainfall were analyzed, and the key thresholds of necessary and approximate sufficiency for short-duration heavy rainfall were obtained. The conclusions are as follows.

(1) Regarding moisture conditions. PWAT is the best indicator for short-duration heavy rainfall: the larger the PWAT, the higher the probability of short-duration heavy rainfall. The second best is specific humidity. Relative humidity could help determine whether or not it is going to rain, but does not indicate rainfall intensity. The denotative meaning of the pseudo-equivalent potential temperature is much better than temperature. PWAT of 28 mm is necessary for short-duration heavy rainfall, while a value of more than 59 mm is approximately sufficient.

(2) Regarding instability conditions. For indices to represent environmental instability favorable for short-duration heavy rainfall, BLI and KI are the best. BLI is more impressive by indicating the environment instability conditions with its sign compared to KI. Three-quarters of short-duration heavy rainfall occurred with BLI less than –1.0, and BLI greater than 2.6 indicated no possibility of short-duration heavy rainfall. Three-quarters of short-duration heavy rainfall occurred with KI greater than 36. A short-duration heavy rainfall event should occur with KI not less than 28.1. However, the BCAPE was not effective enough to distinguish the environment favorable for short-duration heavy rainfall.

(3) Regarding dynamic conditions. The importance of lifting for ordinary precipitation and short-duration heavy rainfall is shown by the divergence of 925 and 850 hPa. Generally speaking, the heavier the rainfall intensity, the stronger the required lifting. About 75% of short-duration heavy rainfall events were accompanied by a negative divergence of both 925 and 850 hPa. The portion for 925 hPa was slightly larger than that for 850 hPa, indicating the 925-hPa divergence was more important. However, it is necessary to consider lifting of multilayers near the land surface. The vertical wind shear did not help distinguish the environment favorable for short-duration heavy rainfall.

The statistics show that it is difficult to find a single parameter or a specific threshold to represent the conditions for short-duration heavy rainfall. A complex forecasting method for short-duration heavy rainfall, combining quantities with clear meanings, should be developed. Many characteristics should be fully considered to improve the prediction of short-duration heavy rainfall. However, by estimating whether extreme conditions are present, forecasters can keep a watchful eye on high risk areas of short-duration heavy rainfall.

Precipitation processes, especially the short-duration heavy rainfall process mainly caused by convective activities, cannot be described linearly. Thus, it is impossible to find a general and sufficient condition to forecast short-duration heavy rainfall. Some approximately sufficient thresholds are given, though there are few observations meeting these thresholds.

The statistics presented here focused on central and eastern China. The climatology of sub-regional precipitation was not considered. Thus, further attention is required to apply these results to specific regions. Due to the limited spatial and horizontal resolution of rainfall observations and NCEP FNL data, the results are only suitable for short-term forecasting of short-duration heavy rainfall. Improvements in forecast accuracy are dependent on the development of numerical prediction models. Combinations of multi-source data are necessary. Knowledge of the structure, cloud microphysical processes, and developing mechanism of mesoscale convective systems are required to ultimately solve the forecasting problems of any validity period in the future.

Acknowledgments. We would like to thank Mr. Sheng Jie and Mrs. Cao Yancha for providing the huge amount of NCEP FNL data.

APPENDIX

Definitions of Parameters and Indices

Calculation of the parameters investigated in this study, which represent instability and/or water content (listed in Table 1), are given here.

(1) Total precipitation water is given by: $\mathrm{PWAT} = \frac{1}{\rho g}\int_{p_0}^{p_1} q\mathrm{d}p$, where ρ represents the density of water, g is the acceleration of gravity, and q is the specific humidity. The integral is performed over a column of unit cross-section extending from the earth's surface p_0 to the pressure level p_1, and the top of the atmosphere is usually 200 hPa.

(2) The temperature difference between 850 and 500 hPa is defined as $\mathrm{DT85} = T_{850} - T_{500}$. This metric is widely used during operations in China and is also known as vertical total (Miller, 1972). DT85 only assesses the instability between 850 and 500 hPa. Since the 850–500-hPa layer thickness increases with increasing temperature, the actual lapse rate is very different in summer and winter.

(3) The lifted index is defined as: $\mathrm{LI} = T_{500} - T'$, where T_{500} is the 500-hPa temperature, T' is temperature of an air parcel after it has been lifted pseudo-adiabatically to 500 hPa from its original level. The widely used best lifted index, BLI, is the same as the most unstable lifted index. Thus, BLI is defined as the LI for a parcel with the temperature, dew-point temperature, and pressure at the level where the equivalent temperature reaches its highest value in the 250-hPa layer above the surface.

(4) The total totals is defined as: $\mathrm{TT}=T_{850} + T_{\mathrm{d}850} - 2T_{500}$, where T_{850} and $T_{\mathrm{d}850}$ are the temperature and dew point temperature at 850 hPa, respectively, and T_{500} is the 500-hPa temperature. TT

is a widely used convective index, which is originally defined by U.S. scientists (Peppler and Lamb, 1989).

(5) The K index (KI) is defined as: $K = (T_{850} - T_{500}) + T_{\mathrm{d}850} - (T_{700} - T_{\mathrm{d}700})$, where T_{850}, T_{700}, and T_{500} are the temperature at 850, 700, and 500 hPa, and $T_{\mathrm{d}850}$ and $T_{\mathrm{d}700}$ are the dew point temperature at 850 and 700 hPa, respectively. The KI increases with decreasing static stability between 850 and 500 hPa, increasing moisture at 850 hPa, and increasing relative humidity at 700 hPa.

(6) The convective available potential energy is defined as CAPE=$\int_{p_{\mathrm{EL}}}^{p_{\mathrm{LFC}}} R_d(T_{\mathrm{vp}} - T_{\mathrm{ve}})\mathrm{d}(\ln p)$, where p_{EL} is the pressure of the equilibrium level (EL), p_{LFC} is the pressure of the level of free convection (LFC), and T_{vp} and T_{ve} are the virtual temperature of the lifted parcel and the environment, respectively. There are many different definitions of convective available potential energy in literature. Here, it is defined as the total amount of work done by the upwards buoyancy force exerted on an air parcel as it is lifted from the LFC to the EL. The so-called BCAPE in this paper is the same as the most unstable CAPE, as the convective available potential energy of a parcel with the temperature, dew point temperature and pressure at the level where the equivalent temperature reaches its highest value in the 250-hPa layer above the surface.

(7) Vertical wind shear SHR = $\boldsymbol{V}_2 - \boldsymbol{V}_1$, where $\boldsymbol{V}_2$ and $\boldsymbol{V}_1$ are the wind vectors of the upper and lower layers. Here $\boldsymbol{V}_1$ is the land surface wind vector. The 0–1-, 0–3- and 0–6-km vertical wind shears are represented by SHR1, SHR3, and SHR6, respectively.

From the formulae for DT85, BLI, TT, and KI, we know that these parameters should not be applied to plateau regions as the temperature of 850 and 500 hPa are used.

REFERENCES

Arakawa, A., 2004: The cumulus parameterization problem: Past, present, and future. *J. Climate*, **17**, 2493–2525.

Bunkers, M. J., 2002: Vertical wind shear associated with left-moving supercells. *Wea. Forecasting*, **17**, 845–855.

Boville, B. A., 1991: Sensitivity of simulated climate to model resolution. *J. Climate*, **4**, 469–485.

Chen Jiong, Zheng Yongguang, Zhang Xiaoling, et al., 2013: Distribution and diurnal variation of warm-season short-duration heavy rainfall in relation to the MCSs in China. *Acta Meteor. Sinica*, **27**, 868–888.

Ding Yihui, 2005: *Senior Meteorology*. China Meteorological Press, Beijing, 309–452. (in Chinese)

Doswell III, C. A., H. E. Brooks, and R. A. Maddeox, 1996: Flash flood forecasting: An ingredients-based methodology. *Wea. Forecasting*, **11**, 560–580.

Fan Limiao and Yu Xiaoding, 2013: Characteristic analyses on environmental parameters in short-term severe convective weather in China. *Plateau Meteor.*, **32**, 156–165. (in Chinese)

Fankhauser, J. C., N. A. Crook, J. Tuttle, et al., 1995: Initiation of deep convection along boundary layer convergence lines in a semitropical environment. *Mon. Wea. Rev.*, **123**, 291–314.

Fritsch, J. M., and R. E. Carbone, 2004: Improving quantitative precipitation forecasts in the warm season: A USWRP research and development strategy. *Bull. Amer. Meteor. Soc.*, **85**, 955–965.

Holloway, C. E., and J. D. Neelin, 2009: Moisture vertical structure, column water vapor, and tropical deep convection. *J. Atmos. Sci.*, **66**, 1665–1683.

Huang Gang, 2006: The assessment and difference of the interdecadal variations of climate change in northern part of China with the NCEP/NCAR and ERA-40 reanalysis data. *Climatic Environ. Res.*, **11**, 310–320. (in Chinese)

Humphreys, W. J., 1919: Intensity of precipitation. *Mon. Wea. Rev.*, **47**, 722.

Lei Lei, Sun Jisong, and Wei Dong, 2011: Distinguishing the category of the summer convective weather by sounding data in Beijing. *Meteor. Mon.*, **37**, 136–141. (in Chinese)

Lei Lei, Sun Jisong, Wang Guorong, et al., 2012: An experimental study of the summer convective weather categorical probability forecast based on the rapid updated cycle system for the Beijing area (BJ-RUC). *Acta Meteor. Sinica*, **70**, 752–765. (in Chinese)

Li Yaodong, Liu Jianwen, and Gao Shouting, 2004: On the progress of application for dynamic and energetic convective parameters associated with severe convective weather forecasting. *Acta Meteor. Sinica*, **62**, 401–409. (in Chinese)

Li Zhinan and Li Tingfu, 2000: Analysis on the environmental conditions and dynamic trigger mechanism

of a severe convective rainstorm in Beijing. *Quart. J. Appl. Meteor.*, **11**, 304–311. (in Chinese)

Lin, Y. L., S. Chiao, T. A. Wang, et al., 2001: Some common ingredients for heavy orographic rainfall. *Wea. Forecasting*, **16**, 633–660.

Lu Hancheng and Yang Guoxiang, 2000: *Theory and Forecasting of Mesoscale Meteorology*. China Meteorological Press, Beijing, 301 pp. (in Chinese)

McBride, J. L., and W. M. Frank, 1999: Relationships between stability and monsoon convection. *J. Atmos. Sci.*, **56**, 24–36.

Miller, R. C., 1972: Notes on Analysis and Severe-storm Forecasting Procedures of the Air Force Global Weather Central. Air Weather Service (MAC), U. S. A. F., Technical Report 200 (Rev.), 183 pp.

Molinari, J., and M. Dudek, 1992: Parameterization of convective precipitation in mesoscale numerical models: A critical review. *Mon. Wea. Rev.*, **120**, 326–344.

Peppler, R. A., and P. J. Lamb, 1989: Tropospheric static stability and central North American growing season rainfall. *Mon. Wea. Rev.*, **117**, 1156–1180.

Qian Chuanhai, Zhang Jinyan, Ying Dongmei, et al., 2007: A severe convection weather of Jiangxi in April 2003. *J. Appl. Meteor. Sci.*, **18**, 460–467. (in Chinese)

Rasmussen, E. N., 2003: Refined supercell and tornado forecast parameters. *Wea. Forecasting*, **18**, 530–535.

Rasmussen, E. N., and D. O. Blanchard, 1998: Baseline climatology of sounding-derived supercell and tornado forecast parameters. *Wea. Forecasting*, **13**, 1148–1164.

Sun Jisong, Dai Jianhua, He Lifu, et al., 2014: *Basic Theory and Technical Methods on Severe Convective Weather Forecasting*. China Meteorological Press, Beijing, 282 pp. (in Chinese)

Thompson, R. L., B. T. Smith, J. S. Grams, et al., 2012: Convective modes for significant severe thunderstorms in the contiguous United States. Part II: Supercell and QLCS tornado environments. *Wea. Forecasting*, **27**, 1136–1154.

Tian Fuyou, Zheng Yongguang, Mao Dongyan, et al., 2014: Study on probability distribution of warm season hourly rainfall with Γ distribution. *Meteor. Mon.*, **40**, 787–795. (in Chinese)

Wang Xiuming, Yu Xiaoding, and Zhu He, 2012: The applicability of NCEP reanalysis data to severe convection environment analysis. *J. Appl. Meteor. Sci.*, **23**, 139–146. (in Chinese)

Watson, A. I., and D. O. Blanchard, 1984: The relationship between total area divergence and convective precipitation in South Florida. *Mon. Wea. Rev.*, **112**, 673–685.

Weisman, M. L., and J. B. Klemp, 1982: The dependence of numerically simulated convective storms on vertical wind shear and buoyancy. *Mon. Wea. Rev.*, **110**, 504–520.

Wetzel, S. W., and J. E. Martin, 2001: An operational ingredients-based methodology for forecasting midlatitude winter season precipitation. *Wea. Forecasting*, **16**, 156–167.

Wilson, J. W., N. A. Crook, C. K. Mueller, et al., 1998: Nowcasting thunderstorms: A status report. *Bull. Amer. Meteor. Soc.*, **79**, 2079–2099.

Yin Dongping, Wu Haiying, Zhang Bei, et al., 2010: Analysis on a severe convective weather triggered sea breeze front. *Plateau Meteor.*, **29**, 1261–1269. (in Chinese)

Yu, X., and T. -Y. Lee, 2010: Role of convective parameterization in simulations of a convection band at grey-zone resolutions. *Tellus A*, **62**, 617–632.

Zhang Jiacheng and Lin Zhiguang, 1985: *Climate of China*. Science and Technology Press of Shanghai, Shanghai, 46–127. (in Chinese)

Zhang Tao, Lan Yu, Mao Dongyan, et al., 2013: Advances of mesoscale convective weather analysis in NMC. I: Convective weather environment analysis and supporting techniques. *Meteor. Mon.*, **39**, 894–900. (in Chinese)

Zhang Xiaoling, Chen Yun, and Zhang Tao, 2012: Mesoscale convective weather analysis and severe convective weather forecasting. *Acta Meteor. Sinica*, **70**, 642–654. (in Chinese)

Zhao Ruixia and Wu Guoxiong, 2007: Water budget for the Yangtze River basin and evaluation of ECMWF and NCEP/NCAR reanalysis data. *Acta Meteor. Sinica*, **65**, 416–427. (in Chinese)

Zheng Linlin, Sun Jianhua, Zhang Xiaoling, et al., 2013: Organizational modes of mesoscale convective systems over central East China. *Wea. Forecasting*, **28**, 1081–1098.